

Adenomatous Polyposis Coli as a Scaffold for Microtubule End-Binding Proteins

Laurence Serre, Virginie Stoppin-Mellet and Isabelle Arnal

Grenoble Institut des Neurosciences, *INSERM U1216, Univ. Grenoble Alpes, Grenoble, 38000 France*

Correspondence to Laurence Serre and Isabelle Arnal: *laurence.serre@univ-grenoble-alpes.fr, isabelle.arnal@univ-grenoble-alpes.fr*
https://doi.org/10.1016/j.jmb.2019.03.028
Edited by E. Nogales

Abstract

End-binding proteins (EBs), referred to as the core components of the microtubule plus-end tracking protein network, interact with the C-terminus of the adenomatous polyposis coli (APC) tumor suppressor. This interaction is disrupted in colon cancers expressing truncated APC. APC and EBs act in synergy to regulate microtubule dynamics during spindle formation, chromosome segregation and cell migration. Since EBs autonomously end-track microtubules and partially co-localize with APC at microtubule tips in cells, EBs have been proposed to direct APC to microtubule ends. However, the interdependency of EB and APC localization on microtubules remains elusive. Here, using *in vitro* reconstitution and single-molecule imaging, we have investigated the interplay between EBs and the C-terminal domain of APC (APC-C) on dynamic microtubules. Our results show that APC-C binds along the microtubule wall but does not accumulate at microtubule tips, even when EB proteins are present. APC-C was also found to enhance EB binding at the extremity of growing microtubules and on the microtubule lattice: APC-C promotes EB end-tracking properties by increasing the time EBs spend at microtubule growing ends, whereas a pool of EBs with a fast turnover accumulates along the microtubule surface. Overall, our results suggest that APC is a promoter of EB interaction with microtubules, providing molecular determinants to reassess the relationship between APC and EBs.
© 2019 Elsevier Ltd. All rights reserved.

Introduction

Adenomatous polyposis coli (APC) is a large tumor suppressor present in all mammalian cells. Mutations of the *APC* gene lead to the loss of its C-terminal domain (APC-C) and have been correlated with neurological disorders and cancer development [1–3]. In cancer cells, a truncated form of APC generates severe cytoskeletal defects, causing disorganized mitotic spindles and abnormal chromosome segregation [4–6]. The APC-C region is an unstructured region that contains the major binding sites for microtubules, actin and end-binding proteins (EBs) [7–9]. EBs are plus-end tracking proteins (+TIPs) that concentrate at microtubule growing (+) ends to control microtubule dynamics and organization. EBs are master integrators of plus-end-tracking complexes since they autonomously track microtubule ends, to which they recruit multiple other +TIPs and proteins [10–12]. The three mammalian EBs (EB1, EB2 and EB3) are dimers. Each EB monomer is composed of a globular N-terminal domain (so-called calponin homology domain or CH domain) that includes a microtubule-binding domain, and a C-terminal domain responsible for the dimerization and constituted by a coiled-coil motif, the EB homology domain (EBH) and a short disordered residue tail [13]. A cavity on the surface of the EBH domain accommodates the SxIP motifs common to several +TIPS such as APC, MCAK or CLASP2 [7]. The key role of EBs in the formation of +TIP complexes at microtubule ends requires a tight regulation of the microtubule-binding properties of EBs. To date, only few inhibitors of EB binding at microtubule ends have been identified [14–16].

Numerous studies have shown that APC and EBs act in synergy to regulate microtubule organization in cellular processes such as spindle formation, chromosome segregation and cell migration [17–19]. APC and EBs contribute to common regulatory pathways of microtubule-end capture and microtubule dynamics. Moreover, APC and EBs co-localize at microtubule ends in cells, which has led to the hypothesis that EBs

© 2019 Elsevier Ltd. All rights reserved.

target APC to microtubule ends [20]. APC and EBs can also independently associate with microtubule ends [21], suggesting alternative mechanisms for their recruitment onto microtubules [21–23]. Although studies into the relationship between APC and EBs have been ongoing for nearly 20 years, the molecular interplay between EBs, APC and microtubules remains elusive. Key issues need to be addressed to understand how the cytoskeleton is regulated by the APC/EB duo, in particular how interaction of APC and EBs influences the properties and localization of each protein with respect to microtubules and its impact on microtubule dynamics.

Here, using TIRF microscopy and single-molecule imaging, we reconstituted the functional interplay between the C-terminal domain of APC (APC-C) and EBs on dynamic microtubules *in vitro*. In our experimental conditions, EBs do not recruit APC-C to microtubule ends, but rather APC-C promotes EB binding both at the end and to the lattice of growing microtubules. This positive regulation depends on direct interaction between APC-C and the C-terminal domain of EBs. This interplay between APC-C and EBs produces highly dynamic microtubules. By identifying APC-C as a promoter of EB-microtubule binding properties, our work provides novel molecular bases from which to reconsider APC/EB interaction in cells, in particular the synergy between APC and EBs in mitosis and how any disruption of this interaction influences cancer emergence or progression.

Results

APC-C stimulates EB recruitment on microtubules

To characterize the cytoskeletal-based functions affected by APC truncation, we investigated how APC-C and EBs together affected dynamic microtubules. To do so, we produced APC-C corresponding to the C-terminal domain (2131–2843) of human APC (Fig. 1). This construct contains the microtubule-binding domain (that overlaps the so-called ANS1 region [8]), a potential dimerization domain (ANS2) [8] and two SxIP signatures recognized by EBs (SRLP and SQIP) [7,25]. We used a TIRF-based functional assay to examine combined APC-C and EB3 activity on dynamic microtubules. APC-C strongly enhanced GFP-EB3 comets in the presence of 100 mM KCl, although at this salt concentration, GFP-EB3 alone only bound very weakly to microtubule ends (Fig. 2 and Movie S1). In line with this result, microtubules assembled in the presence of both proteins grew faster and with nearly 2-fold more catastrophes than microtubules assembled with tubulin alone, due to the polymerization-promoting and catastrophe-promoting

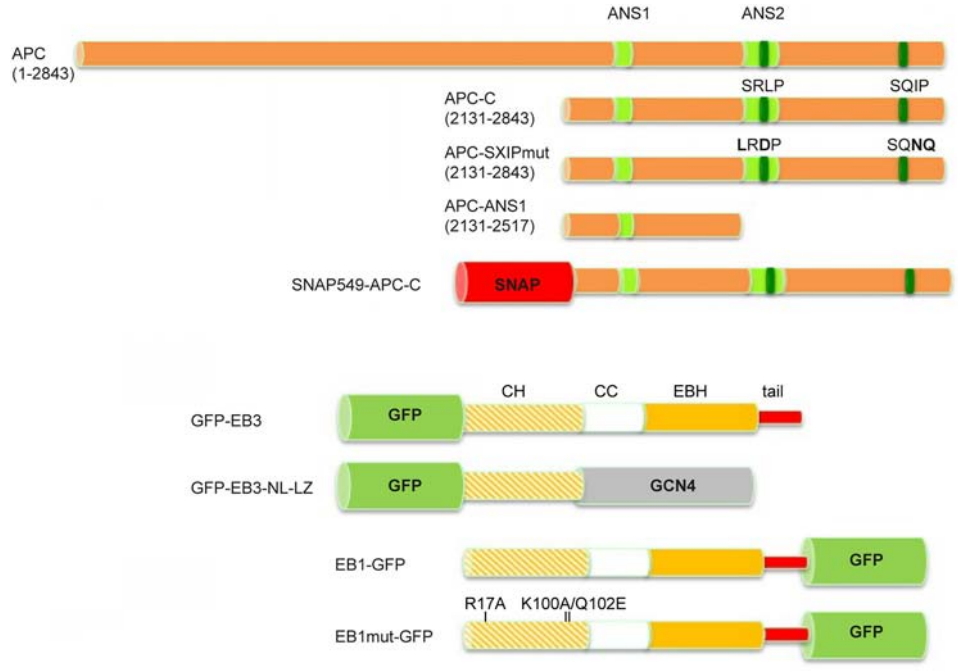


Fig. 1. Schematic view of the proteins used in this study. APC: Bright green: ANS1 and ANS2, two domains involved in actin nucleation [8]. ANS1 overlaps with the microtubule-binding domain [8]. Dark green: SRLP and SQIP represent the two SxIP EB-binding motifs of APC. EB3 and EB1: The different structural domain of EBs are represented. CH, calponin domain; CC, coiled coil domain; EBH, end-binding homology domain; Tail, acidic tail; GCN4, homodimerization domain of the yeast transcriptional activator GCN4 (according to Buey *et al.* [24]).

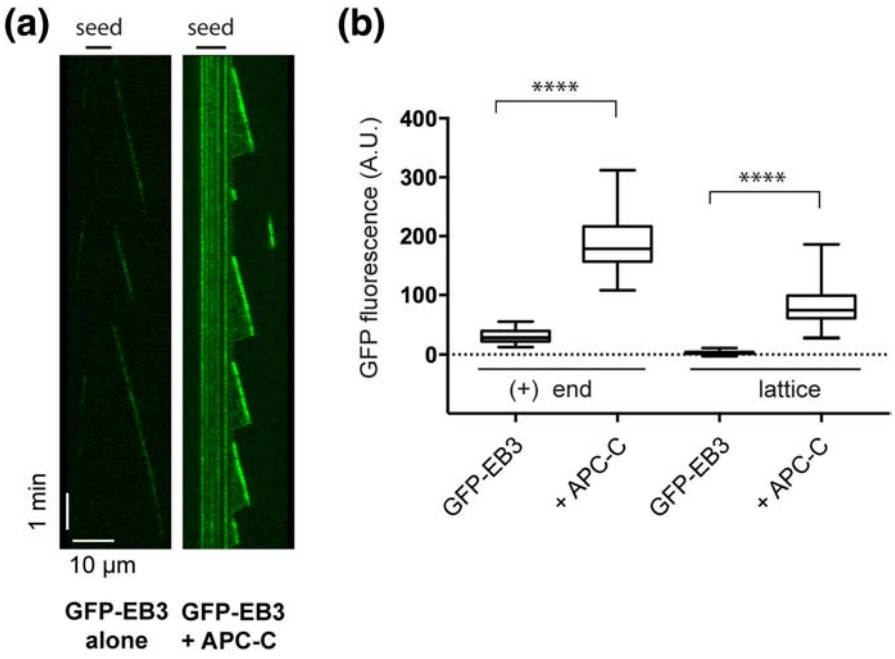


Fig. 2. The C-terminal domain of APC dramatically increases GFP-EB3 recruitment to microtubules. Microtubule nucleation was induced from ATTO-565-tubulin seeds by mixing 15 µM bovine tubulin containing 15% fluorescent ATTO-565-tubulin with either 25 nM GFP-EB3 alone or in the presence of 50 nM APC-C. (a) Representative kymographs showing GFP-EB3 fluorescence on microtubules in the absence and presence of APC-C. (b) Quantification of GFP-EB3 fluorescence at microtubule (+) ends and on the microtubule lattice [number of comets analyzed: n = 42 (GFP-EB3); n = 50 (GFP-EB3 + APC-C)].

activities of APC-C and GFP-EB3, respectively (Table 1). In addition to affecting the microtubule end-tracking properties of EB3, APC-C also increased EB3 binding along the microtubule lattice (Fig. 2). Three hypotheses could explain EB3 accumulation at microtubule ends in the presence of APC-C. First, the large EB3 comets could result from the rapid growth of microtubules, since EB3 comet size is linked to microtubule polymerization rate [26,27]. According to Rickman *et al.* [27], an increase in the microtubule

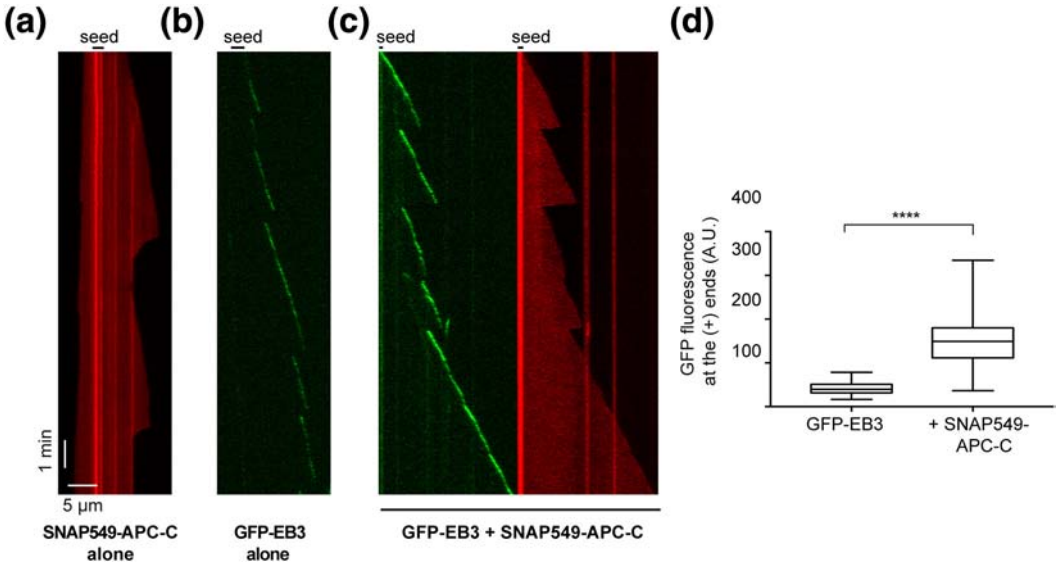


Fig. 3. The C-terminal domain of APC does not accumulate at the microtubule (+) ends. Microtubule nucleation was induced from ATTO-565-tubulin seeds by mixing 15 µM bovine tubulin with (a) 50 nM SNAP549-APC-C alone, (b) 25 nM GFP-EB3 alone or (c) combining the two proteins. Representative kymographs illustrating the distribution of GFP-EB3 and SNAP549-APC-C on microtubules. (d) Quantification of GFP-EB3 fluorescence at microtubule (+) ends [number of comets analyzed: n = 70 (GFP-EB3); n = 95 (GFP-EB3 + SNAP549-APC-C)].

Table 1. Effects of APC-C and EB3 on microtubule dynamic parameters

	Growth rate (SD; μm/min	N	Time (min)	Shrinking rate (SD; μm/min	N	Time (min)	Frequency of catastrophes	N
Tubulin	0.91 (0.20)	116	678	22.5 (7.7)	77	22.3	0.15	101
EB3	1.11 (0.22)	100	600	28.6 (9.8)	55	15.9	0.15	90
APC-C	1.53 (0.30)	122	1076	28.9 (12.6)	77	47.5	0.08	88
APC-C+ EB3	1.64 (0.29)	145	601	20.30 (8.3)	120	49.2	0.24	144
APC-ANS1	1.52 (0.30)	126	1133	29.8 (10.8)	66	42.1	0.07	85
APC-ANS1 + EB3	1.41 (0.26)	223	1995	37 (12.8)	125	56.5	0.09	181

N = number of events; SD, standard deviation.

growth rate about 1.5 times is associated with a 2-fold increase in EB1 comet intensity. In our conditions, a similar increase of the microtubule growth rate (Table 1, EB3/APC-C compared to EB3) is associated with a 10-fold increase in EB3 comet intensity (Fig. 2b). Thus, the increase in microtubule growth rate is insufficient to explain the increase in EB3 comet intensity in the presence of APC-C.

Second, the recruitment of EB3 by APC-C along the lattice could enhance EB3 binding at microtubule ends. Indeed, EB3-GFP fluorescence intensity on the lattice was 5-fold higher in the presence of APC-C, although comet intensity in the same conditions was a full order of magnitude greater (Fig. 2b). Thus, EB3 decoration on the lattice only partially accounts for the strong stimulation of EB3 binding at microtubule (+) ends. Third, EB3 might accumulate at microtubule ends because APC-C preferentially binds this microtubule region. To test this last hypothesis, we determined the distribution of APC-C on microtubules by expressing APC-C fused to a SNAP-tag labeled with the SNAP-Surface-549 fluorophore. On its own, SNAP549-APC-C bound homogeneously throughout the length of growing microtubules (Fig. 3a). Similarly to APC-C (Fig. 2), SNAP549-APC-C promotes GFP-EB3 comets (Fig. 3b–d). No SNAP549-APC-C comet-like accumulation matches GFP-EB3 comets at the microtubule (+) ends, independently of salt concentration or GFP-EB3/SNAP549-APC-C molar ratio (Figs. 3c and S1).

Altogether, these results suggest that APC-C stimulates the recruitment of EB3 to microtubules, while exerting a specific effect on EB3 binding at microtubule (+) ends.

Direct APC-C/EB interaction is required for EB recruitment to microtubules by APC-C

To test whether the enhanced recruitment of EB3 on microtubules involves direct APC-C/EB3 interaction, we used a truncated APC-C form (named APC-ANS1, Fig. 1), which possesses only the APC microtubule-binding domain, and a chimeric EB3-like protein called EB3-NL-LZ (Fig. 1), which exhibits strong end-tracking properties but lacks the native EB C-terminal domain [24]. APC-ANS1 fails to enhance GFP-EB3 recruitment either to the lattice or to the end of elongating microtubules (Fig. 4a–b, Movie S1). The end-tracking pattern for GFP-EB3-NL-LZ on growing microtubules showed a similar pattern alone or when combined with a 50-fold excess of APC-C or APC-ANS1 (Fig. 4c–d). These results demonstrate that APC-C-dependent regulation of EB3 binding on microtubules requires direct interaction between the C-terminal domains of APC-C and EB3. We next mutated the two SxIP sequences of APC-C [7,13,25] and used a sedimentation assay to test their interaction with EB1. In this experiment, we also used a mutant of EB1 (named EB1mut), which cannot bind to microtubules [28]. This combination allowed us to specifically measure APC-dependent recruitment of EBs to microtubules.

Our results indicated that APC-C draws a larger fraction of EB1mut with polymerized tubulin into the pellet than APC-C mutated for either a single SxIP or both SxIP sequences (Figs. 5a–b and S2). We selected the double APC-C mutant (APC-SXIPmut) to test its effect on the GFP-EB3 comets by TIRF microscopy. Mutation of both SxIP motifs strongly reduced APC-C-dependent recruitment of GFP-EB3 to microtubule ends (Fig. 5c–d).

EB's microtubule-binding properties are required for the increase in EB comets but not for EB microtubule lattice decoration by APC-C

The results presented above indicate that direct APC-C/EB interaction is required to enhance EB recruitment to microtubules in the presence of APC-C (Figs. 4 and 5). To determine to what extent the intrinsic microtubule-binding properties of EBs are involved in this process, we next examined the effects of APC-C on EB1mut by TIRF microscopy. These

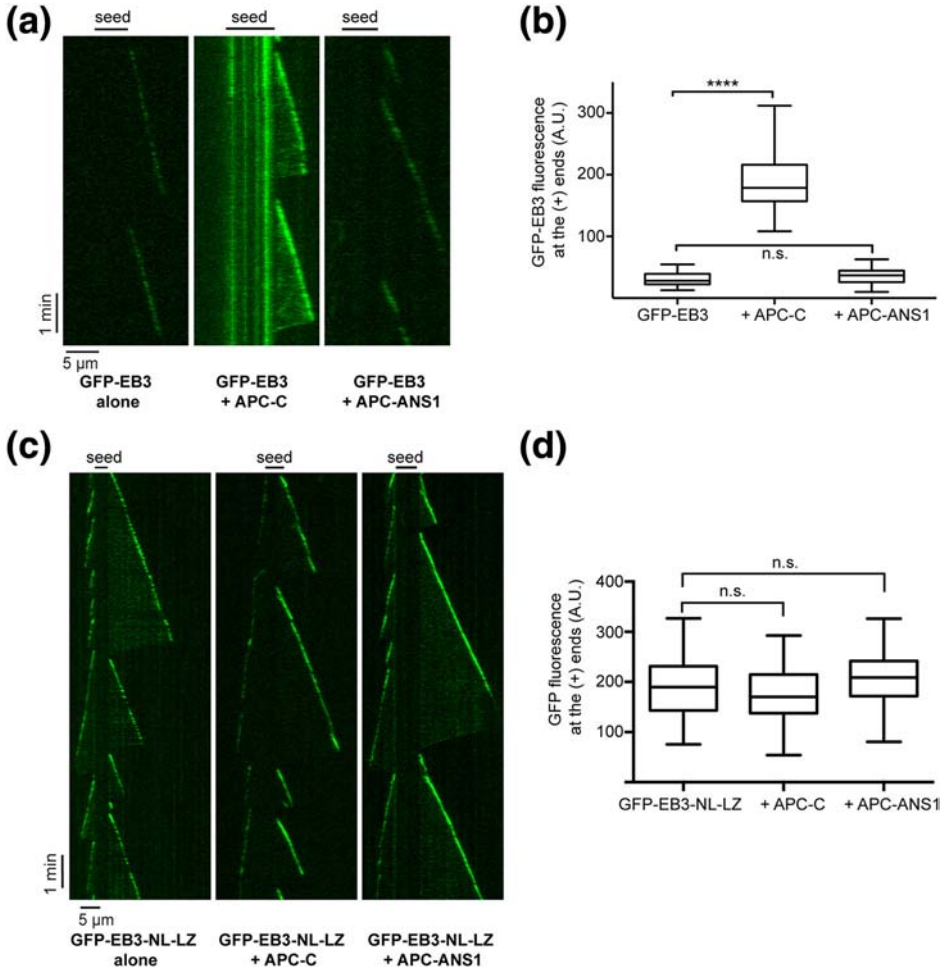


Fig. 4. APC/EB interaction is required for APC-dependent recruitment of EBs to microtubules. Microtubule nucleation was induced from ATTO-565-tubulin seeds by mixing 15 µM bovine tubulin containing 15% fluorescent ATTO-565-tubulin with either 25 nM GFP-EB3 alone or in the presence of 50 nM APC-C (or 50 nM APC-ANS1). (a) Representative kymographs showing GFP-EB3 binding to microtubules alone or in the presence of APC-C or ACP-ANS1. (b) Quantification of GFP-EB3 comet fluorescence in these conditions [number of comets analyzed: n = 39 (GFP-EB3); n = 73 (GFP-EB3 + APC-C); n = 99 (GFP-EB3 + APC-ANS1)]. Microtubule nucleation was induced from ATTO-565-tubulin seeds by mixing 15 µM bovine tubulin containing 15% fluorescent ATTO-565-tubulin with either 1 nM GFP-EB3-NL-LZ alone or in the presence of 50 nM APC-C (or 50 nM APC-ANS1). (c) Representative kymographs showing GFP-EB3-NL-LZ fluorescence on microtubules alone or in the presence of APC-C or APC-ANS1. (d) Quantification of GFP-EB3-NL-LZ comet fluorescence in these conditions [number of comets analyzed: n = 92 (GFP-EB3-NL-LZ); n = 64 (GFP-EB3-NL-LZ + APC-C); n = 69 (GFP-EB3-NL-LZ + APC-ANS1)].

experiments were performed at 50 mM KCl since APC-C-dependent alterations of EB1mut-GFP fluorescence on microtubules were barely detectable at 100 mM KCl. As expected, in these conditions, EB1mut-GFP did not bind microtubules (Fig. 6a). APC-C recruited EB1mut-GFP to the microtubule lattice, and there was no EB1mut-GFP comet-like accumulation at microtubule ends (Fig. 6c–d); in contrast, EB1-GFP efficiently end-tracked microtubules in the presence of APC-C and clearly distinguishable comets were observed (Fig. 6b–d). Thus, APC-C stimulates EB binding to the microtubule lattice without any requirement for direct interaction between EBs and microtubules. However, the increase in EB signal at microtubule ends clearly depends on both EB microtubule-binding properties and APC-C/EB interaction. These results suggest that in those experimental conditions, APC-C recruits EBs to the microtubule lattice and not the other way around. In addition, the mechanisms by which APC-C recruits EBs to the lattice or to the ends of microtubules appear to be distinct.

APC-C has different effects on EB turnover at microtubule ends and on the microtubule lattice

To gain further insight into how APC-C affects the dynamic behavior of EBs on microtubules, we

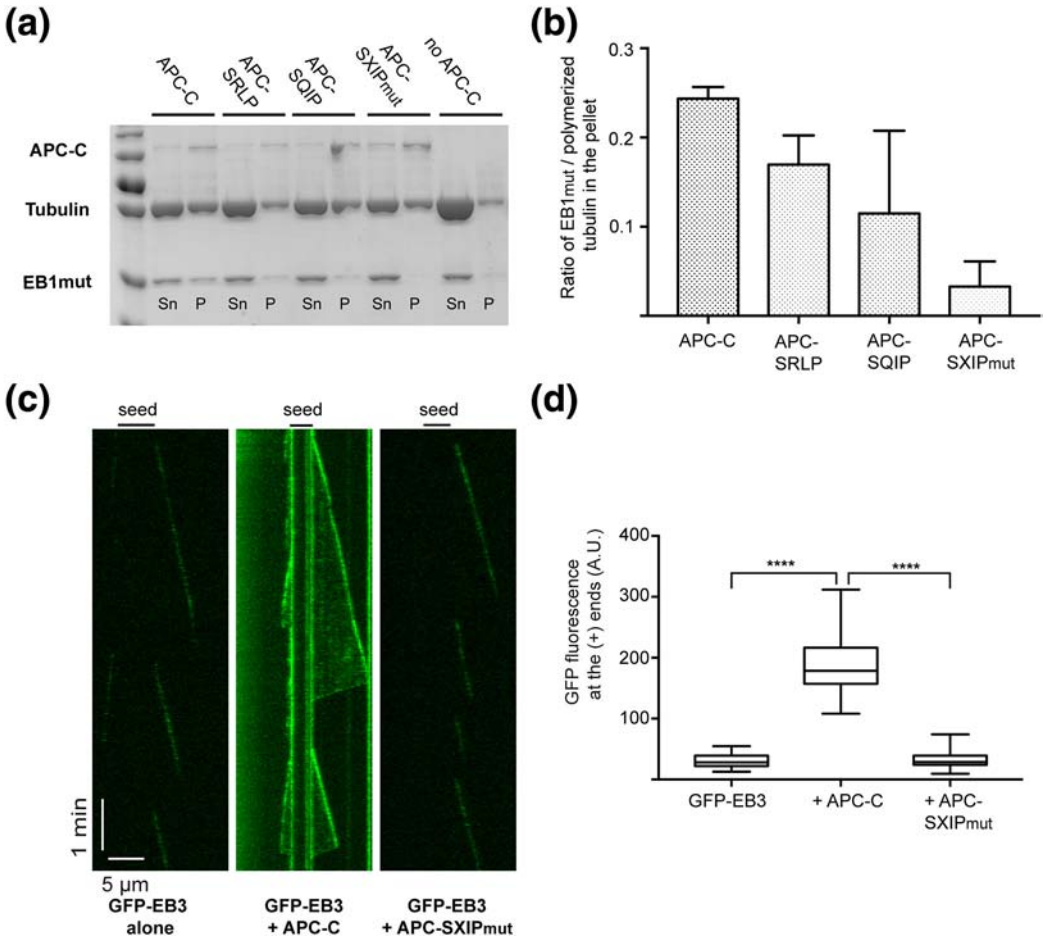


Fig. 5. The SXIP signatures of APC are required for APC-dependent recruitment of EBs to microtubules. (a) Sedimentation assays with dynamic microtubules polymerized in the presence of EB1mut and either APC-C or SxIP-mutated APC-C forms (APC-SRLP, APC-SQIP, APC-SXIPmut). P, pellet; Sn, supernatant. (b) Quantification of the EB1mut band intensities normalized by tubulin in pellet (from three independent experiments). Error bars represent standard deviation. (c) Microtubule nucleation was induced from ATTO-565-tubulin seeds by mixing 15 µM bovine tubulin containing 15% fluorescent ATTO-565-tubulin with either 25 nM GFP-EB3 alone or in the presence of 50 nM APC-C (or 50 nM APC-SXIPmut). Representative kymographs showing GFP-EB3 recruitment to microtubules by APC-C and APC-SXIPmut. (d) Quantification of GFP-EB3 comet fluorescence alone or in the presence of APC-C or APC-SxIPmut [number of comets analyzed: n = 39 (GFP-EB3); n = 73 (GFP-EB3 + APC-C); n = 58 (GFP-EB3 + APC-SXIPmut)].

performed single-molecule TIRF imaging and determined the GFP-EB3 residence time and binding frequency on the microtubule lattice *versus* microtubule (+) end in the absence and presence of APC-C. In line with results from a previous study on EB3 [29], the residence time and binding frequency of GFP-EB3 alone were significantly higher at microtubule ends than on the microtubule lattice, reflecting the greater affinity of EBs for microtubule tips. In the presence of APC-C, the residence time for GFP-EB3 increased about 3-fold at microtubule (+) ends (Fig. 7a–b, Table 2), whereas it was not affected on the microtubule lattice (Fig. 7c–d, Table 2).

In contrast, although the binding frequency of GFP-EB3 was only slightly increased by APC-C at microtubule (+) ends (from 0.046 to 0.077 s^{-1} μm^{-1} nM^{-1} for GFP-EB3 alone and in the presence of 10 nM APC-C, respectively; Table 2), it was significantly increased on the lattice (from 0.00007 to 0.853 s^{-1} μm^{-1} nM^{-1} for GFP-EB3 alone and in the presence of 35 nM APC-C, respectively; Table 2).

From these data, we can conclude that APC-C affects different steps of EB microtubule-binding events depending on where the EBs are bound to the microtubules. APC-C grabs EB3 to the lattice by increasing its binding frequency, but it extends the duration of each EB-binding event at microtubule tips (Fig. 7).

Discussion

APC was described as a tumor suppressor because of its involvement in the β-catenin

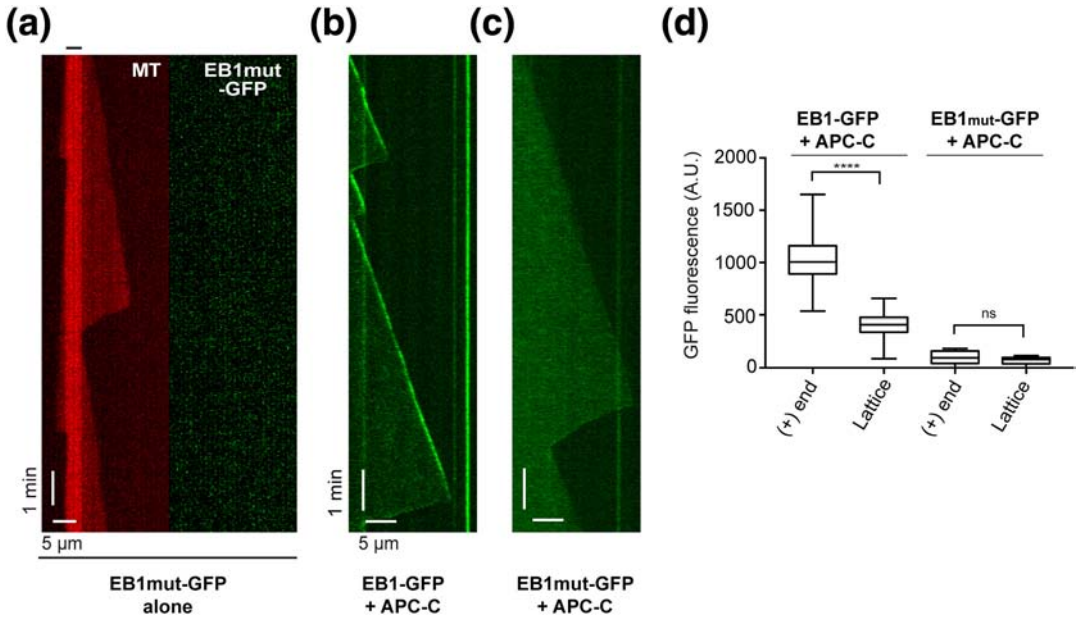


Fig. 6. APC-C can cause a microtubule-binding-incompetent mutant of EB1 to bind microtubules along the lattice. Microtubule nucleation was induced from ATTO-565-tubulin seeds by mixing 12 µM bovine tubulin containing 15% fluorescent ATTO-565-tubulin with 50 nM EB1mut-GFP. (a) Representative kymograph illustrating the absence of microtubule binding of EB1mut-GFP. λ = 561 nm (MT: microtubule) and λ = 488 nm (EB1mut-GFP) fluorescence channels are shown separately. Microtubule nucleation was induced from ATTO-565-tubulin seeds by mixing 12 µM bovine tubulin containing 15% fluorescent ATTO-565-tubulin with 50 nM APC-C and 50 nM EB1-GFP or 50 nM EB1mut-GFP. Representative kymographs illustrating the effect of APC-C on the recruitment of (b) EB1-GFP or (c) EB1mut-GFP to microtubules. (d) Quantification of EB1-GFP and EB1mut-GFP fluorescence on the lattice and at the (+) end of microtubules in the presence of APC-C [number of comets analyzed: n = 35 (EB1-GFP); n = 9 (EB1mut-GFP)].

sequestration complex and in controlling chromosome segregation during mitosis [4,5,9]. APC is a large scaffold protein, and mutations of its gene have been linked to neurological disorders and tumorigenesis [1–3]. Loss of APC function is a major determinant in the development of colorectal cancer [30,31], and, for instance, in the intestinal epithelium, APC mutant cells exhibit reduced directed migration and increased genetic instability [32,33]. In these diseases, stop codons resulting from sporadic or inherited mutations prevent expression of the 3′-terminal region of the *APC* gene, resulting in a truncated APC protein [34]. The deleted C-terminal domain (APC-C) encompasses the major sites known to be involved in cytoskeleton regulation [9,35], in particular binding sites for EBs—master integrators of a complex signaling network at microtubule (+) ends [10–12]. To investigate the EB-related functions of APC that may be lost or affected by truncation of the APC-C domain, we focused this study on interactions between APC-C and EBs, both of which are found at microtubule elongating ends in cells [20,36,37].

Our results show that APC-C greatly enhances the accumulation of EBs on the lattice and at the (+) ends of microtubules (Figs. 2 and 3), suggesting that the regulation of the plus-end tracking proteins network controlled by EBs might be disrupted in diseases linked to APC truncation. We further demonstrated that the increased EB accumulation on microtubules requires molecular interaction between APC-C and EBs, and that removal of the C-terminal residues of APC-C (to produce the APC-ANS1 fragment used in this study) inhibited the formation of GFP-EB3 comets (Fig. 4). These results provide a molecular explanation for those of previous studies with colon cancer cells (SW480 cell line) transfected with APC fragments equivalent to APC-C and APC-ANS1, where shorter EB1 comets were observed when the APC/EB interaction was disrupted [20].

Early studies focused on the regulation and function of APC/EB interaction. Notably, cellular studies proposed that this interaction was essential to target APC to microtubule (+) ends [20,36,38]. However, this conclusion is not straightforward as APC can form clusters at microtubule ends in the absence of EB1 and conversely, EB1 can locate at microtubule tips without co-localizing with APC [21]. APC can also be found in the cell periphery following kinesin-dependent transport along microtubules [22,23], which does not require EB1, thus, different molecular mechanisms contribute to the distribution of EBs and APC at microtubule ends. In this context, our results suggest that APC, without accumulating at microtubule ends, can positively influence the

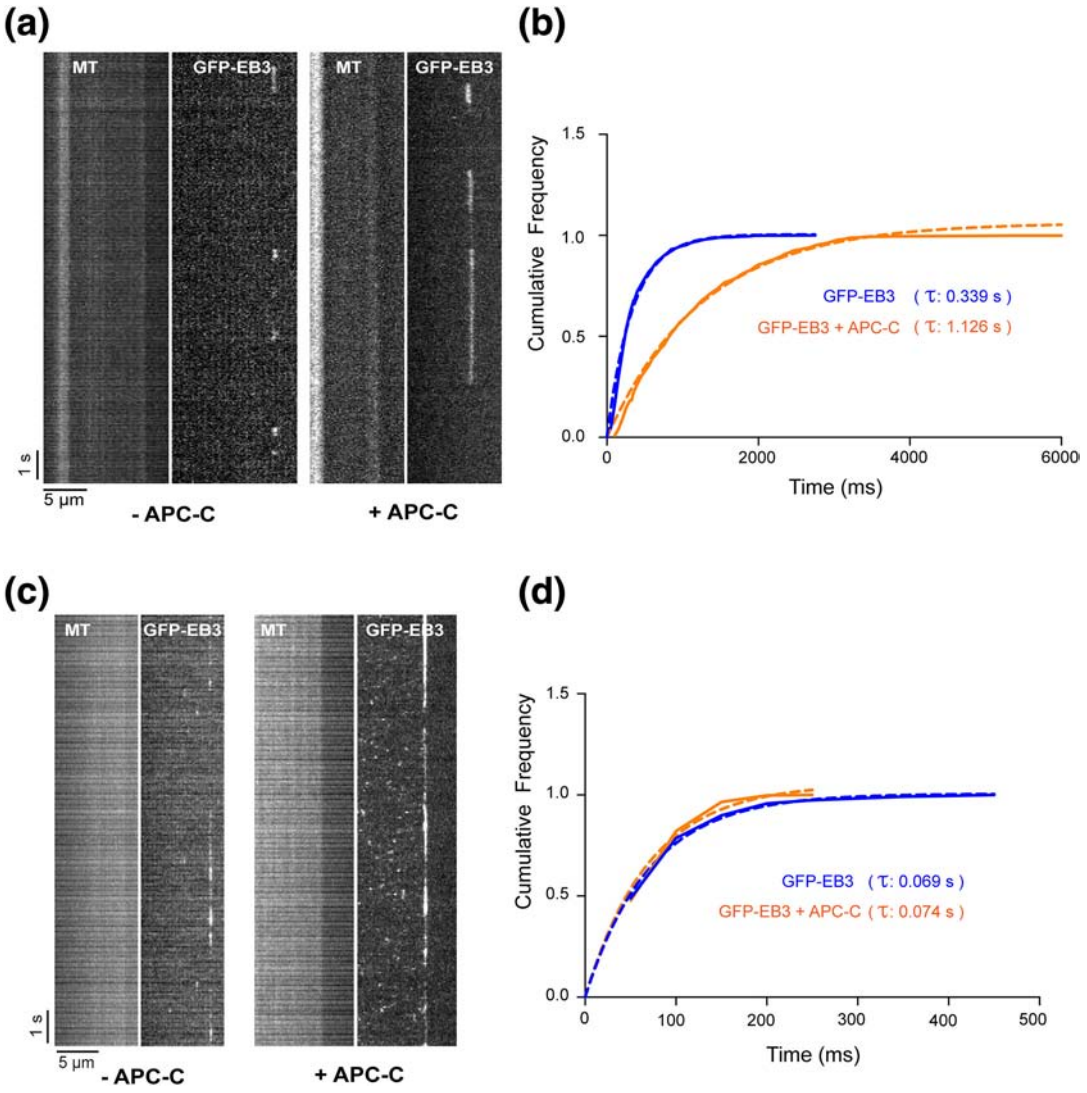


Fig. 7. APC-C promotes differently the recruitment of EBs to microtubule ends and to the microtubule lattice. (a) Representative kymographs showing GFP-EB3 (1 nM) fluorescence at the ends of growing microtubules in the absence or presence of 10 nM APC-C. λ = 561 nm (MT: microtubule) and λ = 488 nm (GFP-EB3) fluorescence channels are shown separately. (b) Cumulative frequency of the residence times measured with 1 nM GFP-EB3 ± 10 nM APC-C. Solid lines and dotted lines represent experimental data and fitting curves, respectively. (c) Representative kymographs showing GFP-EB3 fluorescence on the microtubule lattice in the absence or presence of APC-C. These experiments were performed with either 50 nM GFP-EB3 alone, or 1 nM GFP-EB3 and 35 nM APC-C. (d) Cumulative residence times measured with 50 nM GFP-EB3 alone, or 1 nM GFP-EB3 and 35 nM APC-C. Solid lines and dotted lines represent experimental data and fitting curves respectively.

distribution of EBs on microtubules, in particular by enhancing EB end-tracking properties. Interestingly, APC-C strongly promotes EB3 recruitment to the microtubule surface by drastically increasing the frequency of EB3 binding to the lattice but without altering its residence time (Fig. 7, Table 2). In agreement with these data, we observed that APC-C can cause a microtubule-binding-incompetent mutant of EB1 to bind microtubules along the lattice, suggesting that EB/microtubule interaction is not essential for lattice decoration (Fig. 6). In contrast, at microtubule ends, the increase in EB comets requires both direct APC/EB interaction and EB microtubule-binding properties. APC-C thus appears to promote longer interaction between EBs and microtubule ends by modifying EB conformation and/or altering the microtubule cap recognized by EBs (e.g., rate of GTP hydrolysis, tubulin conformation). Interestingly, the presence of multiple SxIP motifs is used by some +TIPS to enhance their binding to EBs [25,39]. In the case of APC-C, the two SxIP motifs are indeed required to promote EB recruitment to microtubules (Fig. 5) but do not allow

Table 2. Residence times and binding frequencies on microtubules for GFP-EB3 alone and in the presence of APC-C

(+) End	Residence time (s)		Binding frequency (s^{-1} μm^{-1} nM^{-1})	
EB3 1 nM	0.339	N = 959	0.046	N = 64
EB3 1 nM + 10 nM APC-C	1.126	N = 982	0.077	N = 104

Lattice	Residence time (s)		Binding frequency (s^{-1} μm^{-1} nM^{-1})	
EB3 50 nM	0.069	N = 240	0.00007	N = 62
EB3 1 nM + 35 nM APC-C	0.074	N = 750	0.853	N = 56

for APC-C microtubule end-tracking via EB in our experimental conditions (Fig. 3).

Thus, the APC-C-mediated increase in EB comet intensity could be the result of the cumulative effects of (1) the inherent binding properties of EBs at microtubule end, (2) the recruitment of EBs by APC-C along the microtubule surface up to the (+) end, and (3) the long-lived binding of EBs to microtubule ends in the presence of APC-C (Fig. 8).

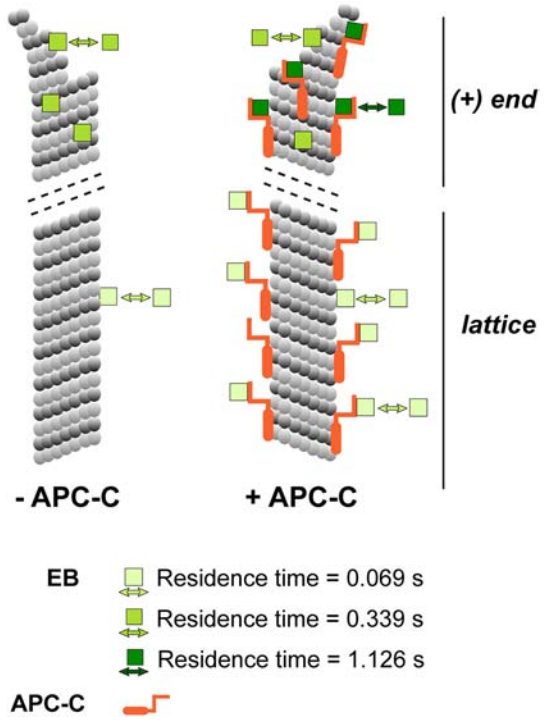


Fig. 8. Schematic representation of EB recruitment by APC-C. In the absence of APC-C, EBs barely bind to the microtubule lattice, and turnover is faster (τ = 0.069 s, represented by pale green arrows) than at microtubule (+) ends (τ = 0.339 s, represented by medium green arrow). This effect results in preferential accumulation of EBs at microtubule (+) ends. Although APC-C binds homogeneously along the microtubule, it promotes the recruitment of EBs to the lattice and to microtubule ends differently. On the lattice, APC-C tethers EBs without changing its turnover (τ = 0.074 s, represented by pale green arrows). At microtubule (+) ends, the increased EB comet signal is the result of slower turnover of EBs interacting with both APC-C and the microtubule (τ = 1.126 s, represented by dark green arrows).

The enhancement of EB comets by APC-C also results in a higher frequency of catastrophes when both proteins are present compared to the frequency recorded with APC-C alone (Table 1). Increasing microtubule catastrophes is a hallmark of *in vitro* EB activity; consequently, APC-C/EB interaction stimulates EB function with regard to microtubule dynamics, which is consistent with a synergistic interaction between EBs and APC regulating spindle dynamics and chromosome alignment during mitosis [17].

Interestingly, in our assay performed at 100 mM KCl, EB3 alone formed very faint comets, whereas bright EB3 comets were visible in the presence of APC-C (Fig. 2). In cells, EB comets are clearly detectable despite the physiological ionic strength, which supports the existence of regulatory mechanisms promoting robust microtubule tracking by EBs. Our results strongly suggest that APC positively regulates EB end-tracking properties.

Finally, the results of this study suggest that APC behaves as a scaffold protein that promotes EB recruitment on microtubules (Fig. 8). APC-C not only extends the lifetime of interactions between EBs and microtubule (+) ends, but also provides a pool of EB molecules with a rapid turnover along the microtubule lattice, which is an unusual substrate for EB proteins [40]. This local increase in EB concentration around the microtubule surface might facilitate rapid accumulation of EB at microtubule tips or could tether specific signaling molecules along the microtubule wall, as suggested previously in neurons [41]. Overall, our results provide novel molecular bases to reconsider the APC/EB synergy in cells.

Materials and Methods

Protein preparation

The APC-C and APC-ANS1 nucleotide sequences were PCR amplified from the human full-length *APC* gene (Life Technologies) for insertion into the pET20b vector (Clontech), which had been opened by digestion with NdeI and HindIII. The SxIP-motif

mutated APC-C proteins (APC-SRLP, APC-SQIP and APC-SXIPmut) were produced by site-directed mutagenesis (Quickmutagenesis kit; Agilent). All these constructs encode proteins labeled with a 6xHistidine motif at the C-terminal extremity. Recombinant proteins were produced in bacteria (BL21-DE3-plysS *Escherichia coli* strain; GE Healthcare), which had been transformed with one of the gene constructs, grown at 37 °C in LB broth supplemented with chloramphenicol and ampicillin. When cultures reached a density of OD_{600} = 0.5, protein expression was induced by adding 0.2 mM IPTG. After 3 h, cells were pelleted, re-suspended in 300 mM NaCl and 50 mM Tris–HCl (pH 7.0) and lysed by several cycles of freezing and thawing. The resulting lysate was centrifuged, and the supernatant containing the over-expressed proteins was incubated with Cobalt resin (Talon; Clontech) at 4 °C. The resin was washed with 300 mM NaCl, 50 mM Tris–HCl (pH 7.0) before eluting the proteins with 200 mM imidazole, 300 mM NaCl and 50 mM Tris–HCl (pH 7.0). Sample quality and purity was improved by performing gel filtration (Superdex-200; GE Healthcare) with 100 mM KCl in BRB80 [80 mM Pipes (pH 6.8), 1 mM $MgCl_2$, 1 mM EGTA] as buffer. Samples were snap frozen in liquid nitrogen and stored at −80 °C.

To produce fluorescent APC-C, the APC-C-6xHis nucleotide sequence was inserted into the pSNAP-tag (T7) vector (New England Biolab) digested with BamHI and XhoI. Expression of the fusion protein was induced by adding 0.2% arabinose (w/v) to an overnight bacterial culture (BL21-AI *E. coli* strain; GE Healthcare) and incubating at 18 °C. The fusion protein was purified as above, but using 50 mM Hepes (pH 7.5), 200 mM KCl and 1 mM DTT as the buffer for the gel filtration step. Labeling with the SNAP549-surface substrate (New England Biolab) was performed according to the manufacturer's instructions at room temperature.

Tubulin and EB proteins used in this study were purified as previously described [42]. The expression vectors for EB3-NL-LZ, GFP-EB3 and EB1-GFP were a gift from Michel Steinmetz [24]. EB1mut (R17A/K100E/Q102E) was generated by site-directed mutagenesis (Quickmutagenesis kit; Agilent).

Oligonucleotides used for mutagenesis are listed in the supplementary material (Table S1).

Co-sedimentation assay

To test the recruitment of EB1mut by SxIP-motif mutated APC-C (APC-SRLP: P2536L/L2538D; APC-SQIP: I2805N/P2806Q; APC-SXIPmut: P2536L/L2538D/I2805N/P2806Q), the following solution was prepared: 15 µM tubulin, 2 µM APC-C (or APC-C mutants), 4 µM EB1mut, 1 mM GTP and 50 mM KCl in BRB80. Twenty microliters of this solution was incubated for 30 min at 37 °C. The mixture was then carefully overlaid on a 40-µL cushion of 60% (w/v) sucrose in BRB80 and 50 mM KCl, before centrifugation at 70,000 rpm (Beckman rotor TLA-100) for 45 min at 35 °C. The protein contents of the supernatant and pellet were analyzed by migration on SDS-PAGE 10% revealed by Coomassie blue staining. The band corresponding to EB1mut was quantified by ImageJ [43].

In vitro microtubule dynamics and microtubule end-tracking assays

To decipher the influence of APC-C and APC-C/GFP-EB3 on microtubule dynamics by TIRF microscopy, flow chambers were prepared and perfused with stable fluorescent (ATTO-565) GMPCPP-microtubule seeds as described previously [42]. Microtubule nucleation was then induced from seeds by adding the following elements: 15 µM bovine tubulin containing 15% fluorescent ATTO-565-tubulin mixed with either 25 nM GFP-EB3 alone or in the presence of 50 nM APC-C in BRB80, 100 mM KCl, 3% (v/v) glycerol, 1 mM GTP, 1% (w/v) BSA, 0.1% (w/v) methyl-cellulose 4000 cp, 4 mM DTT, 1 mg/mL glucose, 70 mg/mL catalase and 580 mg/mL glucose oxidase. Experiments with EB3-NL-LZ were performed using 1 nM EB3-NL-LZ and 50 nM APC-C (or 50 nM APC-ANS1). Samples were observed for 30 min at 32 °C on an inverted microscope (Nikon) equipped with an ilas^2 TIRF system (Roper Scientific), a cooled charged-coupled EMCCD camera (Photometrics) and a warm stage controller (Linkam) and controlled by MetaMorph software. Experiments with EB1-GFP and EB1mut-GFP were performed in 50 mM KCl using 50 nM EB1-GFP (or 50 nM EB1mut-GFP) and 50 nM APC-C. Samples were observed by TIRF microscopy for 30 min at 32 °C as described above. Fluorescence intensity and microtubule dynamic parameters were measured on kymographs using ImageJ software [43] and an in-house KymoTool [14,42].

The fluorescence intensity of EB comets was calculated from the average intensity of a 5-pixel-thick line traced along microtubule growing (+) ends. The same region was used to estimate the background contribution, which was then subtracted from the initial signal. A similar procedure was used to estimate the fluorescence intensity of GFP-EB3 on the microtubule lattice.

Single-molecule assay

For single-molecule TIRF experiments, GFP-EB3 was used at a final concentration of 1 nM in BRB80, 100 mM KCl, 3% (v/v) glycerol, 1 mM GTP, 1% (w/v) BSA, 0.1% (w/v) methyl-cellulose 4000 cp, 4 mM DTT, 1 mg/mL glucose, 70 mg/mL catalase and 580 mg/mL glucose oxidase with or without APC-C. To increase the number of observable events, we used 50 nM GFP-EB3 to estimate the residence time and the binding frequency of GFP-EB3 alone on the

lattice. Data were recorded using a 100× objective and 50-ms exposure time (with streaming acquisition) for 2 min. Microtubule assembly and GFP-EB3 signal were monitored simultaneously using a dual-view system (Roper Scientific). The duration of GFP-EB3 binding events on microtubules (EB3 residence time) were measured on kymographs, both at microtubule (+) ends and on the microtubule lattice. The cumulative distribution of the residence times was fitted by a one-phase exponential decay, applying constraints on Y0 value (Y0 = 0) (Prism7; GraphPad Software). Binding frequencies were determined by dividing the number of binding events by the duration of the recording (in seconds) and by the nanomolar GFP-EB3 concentration over 5 pixels for the (+) end (equivalent to 0.795 μm). For the lattice, the number of binding events per second was considered over the longest dimension of the microtubule, excluding the seed and comet areas. Binding events shorter than our exposure time (50 ms) can be missing, therefore leading to inaccurate residence times for the lattice binding of EB3. Thus, we estimated the accuracy of the residence times (T) by using the mathematical model described in Ref. [44] that allows for fitting-simulated exponential distributions with cutoff. For each residence time (EB3 alone, EB3 + APC-C), we generated 500 simulated samples using the following values: cutoff time = 0.05 s (our experimental detection limit), observation time tobs = 5 s, bin size dt = 0.05 s, residence time T = 0.069 s and T = 0.074 s for EB3 alone and EB3 + APC-C, respectively (Table 2) and a total number of events Ns varying from 50 to 2000. From these data, we drew theoretical graphs of computed mean residence time T and corresponding 95% confidence interval as a function of the number of observed events. Using these graphs, we determined that the residence times have an accuracy of 3 ms for EB3-alone (240 experimental points) and 2 ms for EB3 + APC-C (750 experimental points).

Miscellaneous

Kymographs, intensity estimations and microtubule dynamic parameters were determined using ImageJ software [43]. Contrast of the colored kymographs illustrating the TIRF experiments was adjusted using the ImageJ software according to the following procedure: For each figure panel, the kymographs with the same color channel (λ = 491 nm and λ = 561 nm) were stacked together and the local contrast of the stacked images was enhanced by the "enhance contrast function" implemented in ImageJ using the stack histogram and 0.3% saturated pixels. Statistical analyses were performed using Prism7 (GraphPad Software). The statistical significance was determined using a Kruskal–Wallis test.

Supplementary data to this article can be found online at https://doi.org/10.1016/j.jmb.2019.03.028.

Acknowledgments

We thank Julie Delaroche and Angélique Vinit for technical help, Yasmina Saoudi and Jacques Brocard for their assistance on the imaging facility; Eric Denarier for image analysis; Fabien Boux and Pierre Baraduc for their expertise in statistics; and Annie Andrieux, Anne Fourest-Lieuvin and Sacnicte Ramirez-Rios for helpful discussions. This work was supported by the Institut National pour la Santé et la Recherche Médicale (INSERM; French National Institute for Health and Medical Research) and the Centre National de la Recherche Scientifique (CNRS; French National Centre for Scientific Research) through their joint ATIP-Avenir program, and by the Association pour la Recherche contre le Cancer. This work was supported by the Photonic Imaging Centre at Grenoble Institute Neuroscience (Univ Grenoble Alpes—INSERM U1216), which is part of the IBiSA-certified ISdV core facility.

Competing Interests: The authors declare that no competing interests exist.

Received 30 November 2018;
Received in revised form 28 March 2019;
Accepted 28 March 2019
Available online 6 April 2019

Keywords:
APC;
EB1;
EB3;
microtubule;
TIRF

Abbreviations used:
APC, adenomatous polyposis coli; EB, end-binding protein; +TIP, plus-end tracking protein.

References

[1] T. Onouchi, K. Kobayashi, K. Sakai, A. Shimomura, R. Smits, C. Sumi-Ichinose, et al., Targeted deletion of the C-terminus of the mouse adenomatous polyposis coli tumor suppressor results in neurologic phenotypes related to schizophrenia, Mol. Brain 7 (2014) 21–35.

[2] M. Almuriekhi, T. Shintani, S. Fahiminiya, A. Fujikawa, K. Kuboyama, Y. Takeuchi, et al., Loss-of-function mutation in APC2 causes sotos syndrome features, Cell Rep. 10 (2015) 1585–1598.

[3] I. Näthke, Cancer biology: APC delivers kiss of death to focal adhesions, Curr. Biol. 27 (2017) 805–807.

[4] R.A. Green, K.B. Kaplan, Chromosome instability in colorectal tumor cells is associated with defects in microtubule plus-end attachments caused by a dominant mutation in APC, J. Cell Biol. 163 (2003) 949–961.

[5] N.M. Rusan, M. Peifer, Original CIN: reviewing roles for APC in chromosome instability, J. Cell Biol. 181 (2008) 719–726.
[6] S. Bahmanyar, W.J. Nelson, A.I.M. Barth, Role of APC and its binding partners in regulating microtubules in mitosis, Adv. Exp. Med. Biol. 656 (2009) 65–74.
[7] R.M. Buey, I. Sen, O. Kortt, R. Mohan, D. Gfeller, D. Veprintsev, et al., Sequence determinants of a microtubule tip localization signal (MtLS), J. Biol. Chem. 287 (2012) 28227–28742.
[8] K. Okada, F. Bartolini, A.M. Deaconescu, J.B. Moseley, Z. Dogic, N. Grigorieff, et al., Adenomatous polyposis coli protein nucleates actin assembly and synergizes with the formin mDia1, J. Cell Biol. 189 (2010) 1087–1096.
[9] K. Aoki, M.M. Taketo, Adenomatous polyposis coli (APC): a multi-functional tumor suppressor gene, J. Cell Sci. 120 (2007) 3327–3335.
[10] K.K. Gupta, E.O. Alberico, I.S. Näthke, H.V. Goodson, Promoting microtubule assembly: a hypothesis for the functional significance of the +TIP network, Bioessays 36 (2014) 818–826.
[11] C. Duellberg, M. Trokter, R. Jha, I. Sen, M.O. Steinmetz, T. Surrey, Reconstitution of a hierarchical +TIP interaction network controlling microtubule end tracking of dynein, Nat. Cell Biol. 16 (2014) 804–811.
[12] A. Akhmanova, M.O. Steinmetz, Tracking the ends: a dynamic protein network controls the fate of microtubule tips, Nat. Rev. Mol. Cell Biol. 9 (2008) 309–322.
[13] S. Honnappa, C.M. John, D. Kostrewa, F.K. Winkler, M.O. Steinmetz, Structural insights into the EB1–APC interaction, EMBO J. 24 (2005) 261–269.
[14] S. Ramirez-Rios, E. Denarier, E. Prezel, A. Vinit, V. Stoppin-Mellet, F. Devred, et al., Tau antagonizes end-binding protein tracking at microtubule ends through a phosphorylation-dependent mechanism, Mol. Biol. Cell 27 (2016) 2924–2934.
[15] L. Velot, A. Molina, S. Rodrigues-Ferreira, A. Nehlig, B.P. Bouchet, M. Morel, et al., Negative regulation of EB1 turnover at microtubule plus ends by interaction with microtubule-associated protein ATIP3, Oncotarget 6 (2015) 43557–43570.
[16] E. Tortosa, N. Galjart, J. Avila, C.L. Sayas, MAP1B regulates microtubule dynamics by sequestering EB1/3 in the cytosol of developing neuronal cells, EMBO J. 32 (2013) 1293–1306.
[17] R.A. Green, R. Wollman, K.B. Kaplan, APC and EB1 function together in mitosis to regulate spindle dynamics and chromosome alignment, Mol. Biol. Cell 16 (2005) 4609–4622.
[18] V.M. Draviam, I. Shapiro, B. Aldridge, P.K. Sorger, Misorientation and reduced stretching of aligned sister kinetochores promote chromosome missegregation in EB1- or APC-depleted cells, EMBO J. 25 (2006) 2814–2827.
[19] L. Berrueta, S.K. Kraeft, J.S. Tirnauer, S.C. Schuyler, L.B. Chen, D.E. Hill, et al., The adenomatous polyposis coli-binding protein EB1 is associated with cytoplasmic and spindle microtubules, Proc. Natl. Acad. Sci. U. S. A. 95 (1998) 10596–10601.
[20] J.M. Askham, P. Moncur, A.F. Markham, E.E. Morrison, Regulation and function of the interaction between the APC tumour suppressor protein and EB1, Oncogene 19 (2000) 1950–1958.
[21] K. Kita, T. Wittmann, I.S. Näthke, C.M. Waterman-Storer, Adenomatous polyposis coli on microtubule plus ends in cell extensions can promote microtubule net growth with or without EB1, Mol. Biol. Cell 17 (2006) 2331–2345.
[22] P.T. Ruane, L.F. Gumy, B. Bola, B. Anderson, M.J. Wozniak, C.C. Hoogenraad, et al., Tumour suppressor adenomatous polyposis coli (APC) localisation is regulated by both Kinesin-1 and Kinesin-2, Sci. Rep. 6 (2016) 1–14.
[23] T. Jimbo, Y. Kawasaki, R. Koyama, R. Sato, S. Takada, K. Haraguchi, et al., Identification of a link between the tumour suppressor APC and the kinesin superfamily, Nat. Cell Biol. 4 (2002) 323–327.
[24] R.M. Buey, R. Mohan, K. Leslie, T. Walzthoeni, J.H. Missimer, A. Menzel, et al., Insights into EB1 structure and the role of its C-terminal domain for discriminating microtubule tips from the lattice, Mol. Biol. Cell 22 (2011) 2912–2923.
[25] S. Honnappa, S.M. Gouveia, A. Weisbrich, F.F. Damberger, N.S. Bhavesh, H. Jawhari, et al., An EB1-binding motif acts as a microtubule tip localization signal, Cell 138 (2009) 366–376.
[26] P. Bieling, L. Laan, H. Schek, E.L. Munteanu, L. Sandblad, M. Dogterom, et al., Reconstitution of a microtubule plus-end tracking system in vitro, Nature. 450 (2007) 1100–1105.
[27] J. Rickman, C. Duellberg, N.I. Cade, L.D. Griffin, T. Surrey, Steady-state EB cap size fluctuations are determined by stochastic microtubule growth and maturation, Proc. Natl. Acad. Sci. 114 (2017) 3427–3432.
[28] S.P. Maurer, F.J. Fourniol, G. Bohner, C.A. Moores, T. Surrey, EBs recognize a nucleotide-dependent structural cap at growing microtubule ends, Cell 149 (2012) 371–382.
[29] S. Montenegro Gouveia, K. Leslie, L.C. Kapitein, R.M. Buey, I. Grigoriev, M. Wagenbach, et al., In vitro reconstitution of the functional interplay between MCAK and EB3 at microtubule plus ends, Curr. Biol. 20 (2010) 1717–1722.
[30] L.E. Dow, K.P. O'Rourke, J. Simon, D.F. Tschaharganeh, J.H. Van Es, H. Clevers, et al., Apc restoration promotes cellular differentiation and reestablishes crypt homeostasis in colorectal cancer, Cell 161 (2015) 1539–1552.
[31] T.K. Starr, P.M. Scott, B.M. Marsh, L. Zhao, B.L.N. Than, M.G. O'Sullivan, et al., A sleeping beauty transposon-mediated screen identifies murine susceptibility genes for adenomatous polyposis coli (Apc)-dependent intestinal tumorigenesis, Proc. Natl. Acad. Sci. 108 (2011) 5765–5770.
[32] M.A. Juanes, H. Bouguenina, J.A. Eskin, R. Jaiswal, A. Badache, B.L. Goode, Adenomatous polyposis coli nucleates actin assembly to drive cell migration and microtubule-induced focal adhesion turnover, J. Cell Biol. 216 (2017) 2859–2875.
[33] N. Lugli, V.S. Dionellis, P. Ordóñez-Morán, I. Kamileri, S.K. Sotiriou, J. Huelsken, et al., Enhanced rate of acquisition of point mutations in mouse intestinal adenomas compared to normal tissue, Cell Rep. 19 (2017) 2185–2192.
[34] Y. Miyoshi, H. Ando, H. Nagase, I. Nishisho, A. Horii, Y. Miki, et al., Germ-line mutations of the APC gene in 53 familial adenomatous polyposis patients, Proc. Natl. Acad. Sci. U. S. A. 89 (1992) 4452–4456.
[35] J.B. Moseley, F. Bartolini, K. Okada, Y. Wen, G.G. Gundersen, B. L. Goode, Regulated binding of adenomatous polyposis coli protein to actin, J. Biol. Chem. 282 (2007) 12661–12668.
[36] M. Nakamura, X.Z. Zhou, K.P. Lu, Critical role for the EB1 and APC interaction in the regulation of microtubule polymerization, Curr. Biol. 11 (2001) 1062–1067.
[37] Y. Mimori-Kiyosue, S. Tsukita, "Search-and-capture" of microtubules through plus-end-binding proteins (+TIPs), J. Biochem. 134 (2003) 321–326.
[38] Y. Mimori-Kiyosue, N. Shiina, S. Tsukita, Adenomatous polyposis coli (APC) protein moves along microtubules and concentrates at their growing ends in epithelial cells, J. Cell Biol. 148 (2000) 505–518.
[39] K.W. Fong, F.K.C. Au, Y. Jia, S. Yang, L. Zhou, R.Z. Qi, Microtubule plus-end tracking of end-binding protein 1 (EB1)

is regulated by CDK5 regulatory subunit-associated protein 2, J. Biol. Chem. 292 (2017) 7675–7687.
[40] M. Zanic, J.H. Stear, A.A. Hyman, J. Howard, EB1 recognizes the nucleotide state of tubulin in the microtubule lattice, PLoS One 4 (2009), e7585.
[41] L.C. Kapitein, K.W. Yau, S.M. Gouveia, W.A. van der Zwan, P.S. Wulf, N. Keijzer, et al., NMDA receptor activation suppresses microtubule growth and spine entry, J. Neurosci. 31 (2011) 8194–8209.
[42] S. Ramirez-Rios, L. Serre, V. Stoppin-Mellet, E. Prezel, A. Vinit, E. Courriol, et al., A TIRF microscopy assay to decode how tau regulates EB's tracking at microtubule ends, Methods Cell Biol. 141 (2017) 179–197.
[43] C.A. Schneider, W.S. Rasband, K.W. Eliceiri, NIH image to ImageJ: 25 years of image analysis, Nat. Methods 9 (2012) 671–675.
[44] I.A. Telley, P. Bieling, T. Surrey, Obstacles on the microtubule reduce the processivity of Kinesin-1 in a minimal in vitro system and in cell extract, Biophys. J. 96 (2009) 3341–3353.